HHS Public Access

Author manuscript

Biochim Biophys Acta Biomembr. Author manuscript; available in PMC 2022 August 01.

Published in final edited form as:

Biochim Biophys Acta Biomembr. 2021 August 01; 1863(8): 183621. doi:10.1016/j.bbamem.2021.183621.

Site-selective labeling and electron paramagnetic resonance studies of human cannabinoid receptor CB_2

Alexei A. Yeliseev[*], **Kaeli Zoretich**[1], **Levi Hooper**[2], **Walter Teague**, **Lioudmila Zoubak**, **Kirk G. Hines**, **Klaus Gawrisch**[*]

National Institute on Alcohol Abuse and Alcoholism, National Institutes of Health, Bethesda, MD 20892, USA

Abstract

Integral membrane G protein-coupled receptors (GPCR) regulate multiple physiological processes by transmitting signals from extracellular milieu to intracellular proteins and are major targets of pharmaceutical drug development. Since GPCR are inherently flexible proteins, their conformational dynamics can be studied by spectroscopic techniques such as electron paramagnetic resonance (EPR) which requires selective chemical labeling of the protein. Here, we developed protocols for selective chemical labeling of the recombinant human cannabinoid receptor CB_2 by judiciously replacing naturally occurring reactive cysteine residues and introducing a new single cysteine residue in selected positions. The majority of the 47 newly generated single cysteine constructs expressed well in *E. coli* cells, and more than half of them retained high functional activity. The reactivity of newly introduced cysteine residues was assessed by incorporating nitroxide spin label and EPR measurement. The conformational transition of the receptor between the inactive and activated form were studied by EPR of selectively labeled constructs in the presence of either a full agonist CP-55,940 or an inverse agonist SR-144,528. We observed evidence for higher mobility of labels in the center of internal loop 3 and a structural change between agonist vs. inverse agonist-bound CB_2 in the extracellular tip of transmembrane helix 6. Our results demonstrate the utility of EPR for studies of conformational dynamics of CB_2.

Graphical Abstract

[*] correspondence to: Alexei Yeliseev; yeliseeva@mail.nih.gov, Klaus Gawrisch; klausg@mail.nih.gov.
[1]Present address: The Ohio State University College of Medicine, Columbus OH
[2]Present address: University of Michigan College of Pharmacy, Ann Arbor, MI

Declaration of competing interest

The authors declare that they have no conflicts of interest with the contents of this article.

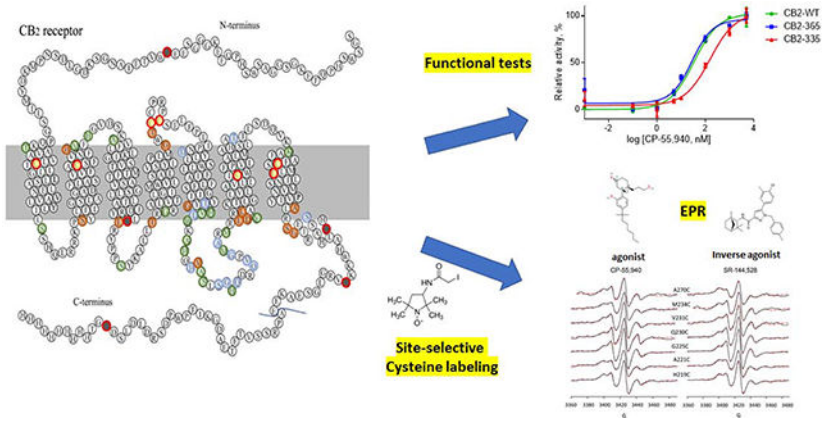

Keywords

Cannabinoid receptor CB_2; EPR; site-selective labeling; GPCR; conformational transition

Introduction

Integral membrane G protein-coupled receptors (GPCR) regulate multiple physiological processes by transducing signals from the extracellular milieu to cytoplasmic proteins and are major targets of pharmaceutical drug development. The recently published X-ray crystal structure of the human cannabinoid receptor CB_2 (1) and a cryo-EM structure of the complex of CB_2 with the G protein (2) have provided insights into the structure of this GPCR at high resolution. (3)

The complex pharmacology of GPCR ligands cannot be fully explained by a small number of alternative static conformations shown by X-ray crystallography (1) and, recently, by cryo-EM (2,3). More dynamic models for ligand regulation of GPCR conformation have been proposed since GPCR display a range of motions associated with their function. Although such protein dynamics are important for both signaling and allosteric regulation, they remain poorly understood. Therefore, additional methods are required to evaluate the ligand-induced conformational changes in GPCR and how the ligand binding affects the conformational dynamics of the receptor.

A proven methodology of examining protein conformational dynamics relies on site-directed spin labeling (SDSL) (4–7). In this technique, a spin label is covalently attached at a specific site by a thiol-reactive tether. This requires that a unique reactive cysteine is inserted into the protein following substitution mutagenesis. Motional freedom of the probe, its solvent accessibility, and distance-dependent interactions between spin-labels have been used to investigate the environment of the protein at the site of spin labeling. (8–11)

To evaluate the SDSL as a tool to study ligand-induced conformational changes in the CB_2 receptor, we generated the “minimal cysteine” construct of CB_2 in which the naturally occurring, reactive, water-exposed cysteine residues were replaced. We demonstrated that the function of this base construct was not compromised, and its performance in ligand-

biding and in G protein-activation tests was similar to the wild type receptor. New cysteine residues were introduced, one at a time, to this base construct at various positions, and their reactivity was studied. The conditions of the labeling reaction were optimized to minimize the contribution of unwanted labeling of the cysteines preserved in the base construct.

To study the conformational dynamics of the intracellular surface of CB_2, we attached nitroxide spin-labels to sites on the intracellular loop 3 (IL3) and the adjacent transmembrane regions (TM5 and TM6) of the receptor. We used EPR spectroscopy to monitor the environment of the spin-label in CB_2 complexes with an inverse agonist SR-144,528 and a full agonist CP-55,940. Significant differences in the efficiency of labeling of these sites along the IL3 and adjacent regions were observed. Furthermore, for a handful of sites, the influence on the EPR label of agonist and inverse agonist-bound conformations of CB_2 was probed. These observations confirm the value of SDSL and EPR methodology for structural studies of the structure of CB_2.

Materials and Methods

CB_2 mutagenesis

The minimal-cysteine mutants of CB_2 were generated as fusions with maltose binding protein as previously described (12). All mutants were obtained from GenScript and contained a His and twin-Streptag required for purification.

CB_2 expression

All CB_2 constructs were expressed in *Escherichia coli* Bl21 (DE3) cultures as previously described (13). Briefly, cells were grown in 2 L batches containing 2YT medium, 0.2% glucose, and ampicillin (50 mg/mL) at 37°C. After reaching optical density of 0.5 (approx. 4 hr. growth), the cultivation temperature was lowered to 20°C and 3 mM (final concentration) of ligand CP-55,940 was added. The recombinant protein production was induced with isopropyl β-D-1-thiogalactopyranoside (0.5 mM). The biomass was collected after 42 hours by centrifugation at 5000 x g for 30 min, washed once with cold PBS and stored at −80°C until use.

CB_2 Purification

Upon partial thawing, cells were resuspended in TBS solution with Complete Protease Inhibitor (no EDTA), DNAse I, and 5mM $MgCl_2$. Cells were lysed using a cell homogenizer (Avestin). Upon homogenization, 10 mM CP-55,940 and Buffer A (2x solubilization buffer: 100 mM Tris-HCl (pH 7.5), 300 mM NaCl, 60% Glycerol; and 10 x Triple detergent solution (1.2% CHS, 10% DDM, 6% CHAPS) were added and the resulting solution was stirred for 1 hr. at 4°C. After stirring, the crude cell extract was centrifuged at 215,000 x g for 1 hr. to separate out the solubilized protein. The supernatant was isolated and applied to Dowex 1×4–50 ion exchange resin for 30 min with orbital mixing at 4°C. The resin was removed from protein solution using a 0.45 mm filter.

The resulting protein extract was further purified using tandem Ni-NTA and StrepTactin XT affinity chromatography. Using FPLC, the protein solution was applied and washed on a

5mL prepacked Ni-NTA column directly followed by a 5mL prepacked StrepTactin XT High Capacity column to capture any non-bound protein from the Ni-NTA column. The protein was eluted from the Ni-NTA resin using imidazole elution buffer (10 mM CP-55,940; Buffer A; 250 mM imidazole) and collected on the StrepTactin XT resin.

Detergent Exchange and Ligand Exchange

Once all protein was bound to the StrepTactin XT column, ligand exchange and detergent exchange were completed. The protein solution was washed with Buffer A supplemented with 10 mM SR-144,528. Detergent was then exchanged from Buffer A to FA buffer (0.5–1.0% DMSO, 0.25 mM Façade-TEG/CHS buffer, 20 mM HEPES; pH. 7.5, 10 mM SR-144,528) using gradient washes. After ligand and detergent exchange, the protein was eluted from the StrepTactin XT column using FA elution buffer (FA buffer with 20 mM biotin). Protein fractions were collected and washed using FA buffer supplemented with SR-144,528, then concentrated. Resulting protein concentration was measured using the DCA protein assay (BioRad Laboratories). The protein was resuspended in FA buffer with 15% glycerol, separated into 200 mg aliquots, frozen in liquid nitrogen, and stored at −80°C.

For protein samples purified with CP-55,940 as the final ligand of interest, the above steps were followed but with 10 mM CP-55,940 in all buffers instead of SR-144,528.

EPR Sample Preparation

A protein aliquot (200 mg; typically, 20–50 mL) was thawed on ice. An FA buffer solution with appropriate ligand (0.5–1.0% DMSO, 0.25 mM Façade-TEG/CHS buffer, 20 mM HEPES; pH 7.5, 10 mM SR-144,528 or CP-55,940) was chilled on ice and degassed under vacuum for 10 min. The FA buffer was briefly removed from vacuum and 0.5 mL was added to the filter column with the protein. The filter column was centrifuged for 7 min at 14 x g at 4°C. After centrifugation, flow through was removed, and washing was repeated three times.

After initial washing, the protein solution (typically 20–30 mL) was removed from the filter and transferred to a 100 mL tube. The volume was adjusted with degassed FA buffer to 40 mL (50 mM CB_2 protein). To this protein solution 1.25 mL of 3-(2-Iodoacetamido)-PROXYL spin label (50 mM stock; final conc. of 1.5 mM in reaction) were added. The protein in the presence of label were incubated together on ice for 30 min.

After labeling was completed, the protein solution was transferred to a fresh 50 kDa molecular weight cutoff (MWCO) filter column. Non-degassed FA buffer (0.5 mL) was added and the filter was centrifuged at 14 x g for 7 min at 4°C to wash out unreacted label. After protein labeling, it was no longer necessary to keep FA buffer under vacuum. This wash process was repeated 9 times to ensure removal of unreacted label. After a final wash, labeled protein was removed from the filter column and protein concentration was measured using the DCA protein assay (BioRad Laboratories).

Performing EPR Measurement and Analysis

After protein labeling, 7 mL of protein sample were transferred to a capillary tube with an inner diameter of 0.8 mm and the tube sealed from both end with capillary tube sealer. EPR

spectra were recorded at 4°C on a Bruker EMXnano spectrometer operating in the X-band frequency range using Xenon software (Bruker). The experiment was run using the following parameters: center of field = 3430 G, field modulation amplitude 2G, sweep width = 150 G, microwave power = 5 mW, sweep time = 60.0 sec., number of scans = 50. The Q-factor of the resonator declined reproducibly after sample insertion to values near 3,000. After measurement, an initial linear baseline correction was performed using the Bruker software.

After acquisition, spectra were analyzed using a fitting procedure from EasySpin/SimLabel (14,15), a MATLAB-based application. Spectra were fitted as superposition of two spectral components with separate sets of parameters. The principal value components A_x and A_y of the nitrogen hyperfine coupling tensor A were set to $A_x = A_y = 6$ G, and the Lorentzian contribution to line broadening of resonances was set to 2 G. It was assumed that hyperfine splittings Ax = Ay = 6 G, and Lorentzian Broadening of resonances was set to 2 G. The weight of spectral components 1 and 2, rotational correlation times assuming an isotropic rotational model, the g factor matrix, hyperfine coupling tensor value Az, and the Gaussian contribution to line broadening of resonances were allowed to vary until a reasonably low root mean square deviation between experimental and fitted spectra was reached which typically required several thousand iterations. A variable Gaussian contribution to linewidth was chosen to account for variability in protein structure as well as for signal superposition from background labeling. An interpretation of components of the g-factor matrix is not prudent due to limitations from signal superposition and limitations of applicability of the isotropic rotational model of label motions.

All spectra were fitted beginning from the same set of initial fit parameters. Fitting was conducted using the Nedler/Mead simplex algorithm, target = derivative, scaling = “scale & linear baseline (lsq1)”, startpoint = center of range. The SimLabel fit generates numerical values of EPR parameters related to the shape of the spectra that were used for analysis. The spectral fitting to an isotropic rotational diffusion model was primarily used to derive the weights of two individual spectral components. The actual motion of the nitroxide label is likely to be anisotropic and, therefore, rotational correlation times and g-factor components reported should be considered only as estimates.

Final linear baseline correction of experimental spectra was conducted with a fitting routine written for Sigmaplot 14 (Systat Software) using the fitted spectrum as reference. Label concentration in samples was determined by double integration of the baseline corrected spectra. Reproducibility of double integration for repeated acquisition of spectra using the same sample was ±10% or better. Absolute concentrations of label were determined by calibration of integral intensity using samples with a known concentration of label.

Results

Development of a minimal cysteine construct of CB_2

The amino acid sequence of the human CB_2 receptor contains 13 cysteine residues, eight of which are believed to be localized in the water-exposed domains of the protein (Supplemental Fig. S1). The residues in positions 174 and 179 of the extracellular loop 2

form an essential disulfide bridge. Preliminary studies demonstrated that several of the remaining cysteine residues in water-exposed regions of CB_2 may interact with sulfhydryl-reactive spin labeling reagents. Consequently, labeling of the wild type CB_2 protein with a nitroxide spin-label produces a complex signal due to contributions from several labeled sites (results not shown). To reduce the complexity of the EPR signal, we systematically replaced the naturally occurring cysteine residues in CB_2 with either serine or alanine.

To examine the structural and functional consequences of such replacements, the wild type and variant constructs were expressed in *E. coli* cells as fusions with the N-terminal maltose-binding protein (MBP) at conditions that favor the formation of functional CB_2 (16). The expression levels of these constructs were analyzed by a Western blot of the whole-cell membrane fraction (Supplemental Fig. S2), and the functional activity by the G protein activation (GEF) test. (17) We found that the replacement of six cysteine residues in the water-exposed sites of the receptor with serine in construct CB_2-365 (C(4, 134, 175, 313, 320, 360)S) did not affect the activation of the receptor by the agonist CP-55,940 (results not shown). On the other hand, a replacement of several of the TM-localized cysteines (construct CB_2-C335, C(4, 40, 89, 134, 175, 288, 313, 320, 360)S, C284A) significantly reduced the potency of the agonist CP-55,940 as revealed by the G protein activation (GEF) test (Fig.1). EC_{50} for CP-55,940 for the WT and CB_2-365 constructs were 13 nM while for CB_2-335 – 95 nM, likely due to the reduced binding of the agonist by the variant CB2–335 in which most of the cysteine residues in TM domains have been replaced.

Based on these observations, the minimal cysteine construct CB_2-365 was selected for subsequent optimization. The TM-located cysteine residues are presumed to be less reactive toward the water-soluble spin-labels and, therefore, are somewhat less likely to contribute to the EPR signal. We will demonstrate below that although such TM-localized cysteines are likely to be less-reactive, they still contribute significantly to the overall labeling, thereby complicating signal analysis.

Furthermore, the C-terminus of CB_2 was truncated at position 331 to favor the formation of a monomeric receptor in detergent micelles, to generate CB_2-365/C331 (Supplemental Fig. S1). Our preliminary results indicate that oligomerization in detergent micelles may adversely affect the homogeneity of the purified CB_2 sample. However, there are numerous reports of truncations of N- and C-termini used to improve the homogeneity of GPCR preparation for high resolution structural studies (18–21). We therefore tested several variants of CB_2 truncated at N- and C-termini for their expression in *E. coli* and activity in GEF tests. Several constructs truncated at N-termini downstream of amino acid 5 showed reduced expression and/or activation in GEF tests, and therefore were not used in subsequent trials. Likewise, the truncation of large parts of the C-terminus of CB_2 reduced the functionality of the receptor. On the other hand, the CB_2 construct truncated at C-terminus after amino acid 331 expressed well in *E. coli* and its functional activity was not affected (Supplemental Fig. S3). Furthermore, the purified CB_2-365/C331 protein eluted predominantly as a monomer in size-exclusion chromatography analysis (Supplemental Fig. S4). Therefore, this construct was selected for subsequent introduction of single cysteine replacements and labeling with the nitroxide spin-label. For simplicity, this truncated variant

is referred to as CB_2-365 since it performed virtually identically to the full-length receptor in expression and functional activity tests.

To generate single cysteine variants of the CB_2-365 construct, the amino acid residues at targeted sites were systematically replaced with cysteine, one at a time. These new residues were placed either at the ends of TM domains or in the cytoplasmic loops of the receptor since these locations are expected to be involved in conformational changes of the receptor in response to ligand binding. The constructs harboring the newly introduced residues were expressed as a fusion with MBP in *E. coli* cells, and their expression levels and functional activity characterized (Fig. 2 and Supplemental Table. S1).

More than half of the 47 single cysteine constructs were expressed in *E. coli* cells at levels similar to that of WT CB_2, and exhibited only slightly reduced activity in the GEF test, as illustrated by the green and blue circles in Fig. 2. Therefore, these constructs were selected for labeling by the sulfhydryl-reactive spin label (Fig. 3). Some of the remaining single cysteine constructs exhibited a significantly diminished functional activity (marked by brown circles in Fig. 2) that precluded their subsequent characterization by EPR.

Optimization of spin labeling conditions

The optimization of labeling conditions was performed for single cysteine replacement constructs, by comparing them to the minimal-cysteine construct CB_2-365. For initial tests of labeling efficiency, the S-(1-oxyl-2,2,5,5-tetramethyl-2,5-dihydro-1H-pyrrol-3-yl)methyl (MTSL) methanesulfonothioate was used. This sulfhydryl-labeling reagent forms a disulfide bond upon reaction with cysteine groups of the protein. However, the product of this reaction is redox-sensitive, releasing the nitroxide spin labels over time (22). To avoid such undesirable degradation, in this study we used the 3-(2-Iodoacetamido)-2,2,5,5-tetramethyl-1-pyrrolidinyloxy (IA-Proxyl) to introduce a spin-label into the protein. While the IA-Proxyl is somewhat less reactive compared to MTSL, it forms a stable C-S bond upon reacting with the SH group of the cysteine, which is not a subject of degradation at experimental conditions (Supplemental Fig. S5).

Due to the large number of constructs studied in this work, it was essential to design a robust and efficient CB_2 protein expression and purification protocol. The receptor is expressed as a fusion with the N-terminal MBP in *E. coli* and purified by two successive steps of affinity chromatography as described in Experimental Procedures. To simplify the purification protocol and to minimize the number of steps, the MBP fusion partner was not removed from the receptor. The MBP does not contain cysteine residues and therefore was inert in the reaction with nitroxide spin label. Furthermore, the presence of MBP appears to add to the stability of CB_2 in detergent solutions (unpublished observations). The last step of purification of the receptor was performed in the presence of Façade-TEG detergent that, due to its low aggregation number, forms small micelle particles. A significant difference in sizes between the CB_2-containing micelles and the empty Façade-TEG micelles allows their efficient separation in spin-concentrators and concentrating of the purified protein without significant co-concentration of detergent. Furthermore, such size difference made it easy to remove the excess labeling reagent and other small size molecules from protein sample by several rounds of concentration on a spin concentrator equipped with an appropriate filter,

with good recovery of the protein. The purity of protein samples was routinely assessed by SDS-PAGE and Western blot analysis as shown in Supplemental Fig. S6. Partial, spontaneous cleavage of the fusion protein that is sometimes observed in the course of purification is not problematic since the released receptor protein is sufficiently stable at experimental conditions.(17)

The labeling conditions of several representative constructs of CB_2 were optimized to decrease the off-target labeling of undesired sites on the proteins. Because the minimal cysteine CB_2-365 construct contains several functionally critical cysteine residues, it was important to minimize the unwanted labeling of these sites. Thus, a variety of IA-Proxyl labeling conditions were tested, aiming to reduce labeling of the base construct while achieving sufficiently high labeling of the targeted cysteine residue. Initial optimization trials have shown that the traditional approach to labeling involving prolonged incubation of the receptor with the labeling reagent (23–25) resulted in high levels of off-target labeling in several CB_2 mutants (results not shown). Therefore, we chose to perform spin labeling reactions at a high label- and protein concentration over a short period of time, taking advantage of the differential reactivity between the target cysteine and the background cysteine residues present in the base construct. Furthermore, due to the low stability of CB_2 in detergent solutions, all procedures with purified receptor, including the labeling reaction, were performed at 4°C or on ice. We found that 1:25 protein to IA-Proxyl ratio with a 30 min incubation time at 4°C was most effective for sufficiently high labeling of targeted cysteine residue and low off-target labeling.

The EPR experiments on the minimal cysteine-mutant series began with 50 individual protein mutants stabilized by inverse agonist SR-144,528. Upon measurement of all constructs in the series, samples with spectra that did not meet inclusion criteria were eliminated from the analyzed data set. One criterion for removal was labeling efficiency of each protein construct, expressed in units of label/protein, compared to values for the CB_2-365 construct that has no added cysteines. Samples were included for analysis if they labeled at least 30% higher than the CB_2-365 construct. Five samples were removed because they labeled lower, suggesting that the added cysteine was not accessible for labeling. Additionally, spectra were inspected for low signal-to-noise, upon which five additional samples were removed. The final data set included 41 unique protein constructs. A subset of protein mutants was investigated bound to full agonist CP-55940. For this subset, all spectra are shown, independent of background labeling.

EPR of IL3 SR-144,528-bound receptor

To estimate the background signal contribution, all constructs in the minimal-cysteine mutant series were labeled and purified in the presence of an inverse agonist SR-144,528, and their EPR spectra were compared to the spectra of CB_2-365-base construct. The EPR fitting protocol generates a variety of numeric variables that provide valuable structural information about the labeled site (see Methods). Specifically, we focused on the following parameters that characterized significant variation between spectra of the labeled constructs: labels per protein, and content of spectral immobilized Component 1 (C1) fraction, and spectral more mobile Component 2 (C2) fraction. Furthermore, we analyzed rotational

correlation times, and hyperfine coupling tensor value A_z for both spectral components (Supplemental Figures S7–S12).

The labeling efficiency of the constructs in the series of samples covering the IL3 and adjacent tips of TM domains varied significantly. As shown in Figure 4, all represented samples have a labeling efficiency significantly above the base construct (label/protein = 0.15). This suggests the successful, partial labeling of the site of interest in each variant construct, with a background from residual reactivity of off-target sites, - since these constructs only differ from CB_2-365 by a single cysteine addition. The label per protein value represents a valuable parameter characterizing reactivity of cysteine residues placed at different sites of the receptor. Not surprisingly, the highest values were observed for several residues located at water-exposed sites on the receptor, specifically several positions in the IL3 such as H219C and M237C (Fig. 4). Additionally, several other sites, including extracellular tips of transmembrane domains, were also highly reactive (Supplemental Fig. S7).

The C1 component of the EPR spectra represents the more immobilized conformation of the labeled site, while C2 represents the more mobilized one. Two superimposed spectral components originating from the same labeled cysteine result from long lived (10^{-7} s) conformers of cysteine sidechains. By comparing the C2/C1 ratio as determined by the spectral fitting procedure, differences in mobility of each labeled site within the experimental series can be determined (Figure 5). Higher values reflect greater overall mobility of the label, which can then be extrapolated to the mobility of the residue of interest. As shown in Fig. 5, the mobility fluctuates depending on the location of the label. In particular, the residue G225C has a substantially larger C2/C1 value indicating that this site located at the center of IL3 has significantly higher mobility compared to the rest of the loop. Not surprisingly, the C2/C1 value for residues immediately surrounding G225C trend upward as well, indicating that mobility in this region is increased due to structural flexibility. The values of hyperfine splitting A_z of spectral component 1 tends to be higher for labeled sites near the center of IL3 also, suggesting that labels are more water exposed (Fig. S10).

Comparison of CP-55,940- and SR-144,528-bound conformations of CB_2

Binding of an agonist CP-55,940 or inverse agonist SR-144,528 induces significant conformational changes in CB_2 as reported by the recently published X-ray(1) and cryo-EM (2,3) structures. However, the conformational flexibility of IL3 was not examined in these studies. In fact, IL3 was removed from the expression construct described in the X-ray structure of an inverse agonist-bound CB_2, in order to achieve greater rigidity of the protein construct. Since the structure of the intracellular surface of CB_2 including the IL3 is critical for understanding the mode of binding of the G protein (3), in this study we compared EPR spectra of CP-55,940-bound- and SR-144,528-bound receptor for select residues within the IL3 and residue A270C in the extracellular tip of transmembrane helix 6 (Fig. 6, 7 and Supplemental Table S2). Labeling of protein bound to CP-55,940 was generally lower compared to labeling of protein bound to SR-144,528. Therefore, constructs Q230C, V231C and M234C may have low labeling of mutated sites in the presence of CP-55,940 (see Fig.

S7). Furthermore, a A270C site at the extracellular tip of TM6 was added to this comparison.

Significant changes in the appearance of spectra of these constructs, bound to agonist vs. inverse agonist, suggest changes in the chemical environment of the label at this site of the receptor (Fig. 7a). These spectral changes can be quantified using the differences in weight of Component 1 and 2 as previously discussed. From the C2/C1 ratios, one can determine the mobility of the labeled site (Fig. 7c). There is a trend of higher ratios for the center of IL3 from residues H217C to H226C (Fig. 5) suggesting higher mobility in this region. Out of the 7 resides for which ligand effects were investigated, residue A270C at the tip of helix 6 is more mobilized when bound to CP-55,940 (Fig. 7c).

Discussion

The recent reports of the X-ray and cryoEM structures of CB_2 provide valuable starting points for rational design of specific pharmaceuticals targeting this receptor.(1–3) However, much remains to be discovered about the factors and mechanisms involved in activation of CB_2 and its binding with G protein and other cellular interacting partners. In this report we demonstrate that the dynamics of conformational changes of CB_2 can be successfully measured by spectroscopic methods such as EPR.

Site-selective labeling of proteins with nitroxide spin-label for EPR analysis is typically performed by targeting cysteine residues that either are already present in the native receptor or are introduced by genetic manipulations. However, due to the large number of cysteine residues in the WT CB_2, selective labeling of this protein presented a significant challenge. We performed an extensive site directed mutagenesis-based screening of variants of CB_2 receptor in which one or more of the naturally occurring reactive cysteine residues were removed. By coupling this screening with expression and functional characterization of variant receptors, we selected a construct CB_2-365 in which only two functionally essential cysteine residues in water-exposed parts of the protein remained. Replacement of cysteine residues in TM domains of CB_2 was deemed unwarranted since it diminishes ligand binding affinities and negatively affects the activation of the receptor (unpublished observations).

The minimal cysteine construct CB_2-365 was used as a base upon which to introduce new cysteine residues, one at a time, at selected positions on the receptor. Among almost 50 constructs tested, more than half performed reasonably well in expression- and functional activity tests and were selected for subsequent nitroxide spin-labeling. These sites spanned the intra-cellular as well as extra-cellular regions of the receptor, clustering around the ends of transmembrane domains and flexible cytoplasmic loops.

The reaction conditions were optimized to minimize the incorporation of the label into the base construct, and to avoid the degradation of the receptor.(17) Importantly, the labeling as well as EPR measurements were performed in Façade-TEG detergent supplemented with cholesterol derivative CHS (see Methods) to stabilize the receptor (17). The low aggregation number of Façade-TEG allows concentrating of the protein sample in spin-concentrators without accompanying co-concentration of the detergent. Furthermore, the unreacted spin-

label can be easily removed on a centrifugal spin-concentrator with high protein recovery and without any detrimental effects on the protein sample.

We observed significant differences in labeling efficiency of cysteine residues introduced at different sites of the receptor. At our reaction conditions, these differences should parallel reactivity of these residues with sulfhydryl reagents. The highest reactivity was observed for the residues located in more flexible parts of the protein including middle of the IL3 although several other residues located at tips of transmembrane domains also exhibited high reactivity. These data may prove useful when selecting sites for double labeling of CB_2 for distance measurements in by double electron-electron resonance (DEER) experiments.(26) The technique has been used successfully for distance measurements in proteins including GPCR.

Even though the incorporated spin-label was located at water-exposed sites to yield high labeling efficiency, the background contribution from labeling of the base construct CB_2-365 was still significant. The experimental data reported in the figures are therefore a composite of properties from several labeled sites, with comparable or dominating contributions from the site of the introduced mutation. Because of the contribution from background, presumably originating from several sites, the fit parameters should be interpreted as trends with contributions from the site where a cysteine was introduced. From our extensive optimization attempts, it appears unlikely that the current labeling strategy can be improved further. While we have not studied the source of the background signal, we consider it likely that it derives in part from both TM-localized spin labels as well as from partial labeling of the two water-exposed cysteines involved in the formation of the disulfide bridge. This disulfide bridge was previously shown to be essential for preservation of the functional structure of CB_2, and therefore introduction of the spin-label would most certainly result in unfolding of the part of the labeled receptor (17).

In this study, in order to reduce the background labeling while preserving protein function, we intentionally under-labeled our protein constructs, at a rate of about 30% labeling efficiency. However, our labeling procedures can be easily modified by increasing the reaction time, to achieve close to 70–80% label incorporation (1:1 ratio of label per protein). This would be required to generate significantly double-labeled constructs for subsequent DEER measurements. For successful DEER measurements, it is essential that the pair of cysteine residues is labeled predominantly while the non-specific background label incorporation is minimized.

In addition to demonstrating variation in labeling efficiency and reactivity, of mutants in the IL3, we also observed differences in EPR labeling between CB_2 mutants when bound to SR-144,528 or CP-55,940. Notably, the EPR method described here shows a proof of concept for identifying specific changes in mobility and residue-reactivity of CB_2 due to ligand type. Such observations may prove to be a useful starting point for studying conformational changes associated with ligand binding to the receptor, including the IL3, for which data are not available from current X-ray and cryo-EM analysis (1,3). The significant differences between the inactive (SR-144,528-bound) and active (CP-55,940-bound) conformations at the tip of transmembrane helix 6 of the receptor reported here reveal a

concept for structural analysis of CB_2 at additional residues, and could potentially be used for evaluating structural changes induced by other CB_2 ligands.

Conclusions

While much of the present work was devoted to selection and minimization of labeling of a minimal cysteine construct named CB_2-365, the contribution from the labeling of this construct to the EPR signal is still significant. It is possible that at least part of the background signal derives from a partially unfolded fraction of the protein that contains cysteine residues exposed for interaction with nitroxide spin-label. One of the future directions of our work involves expression of single cysteine constructs of CB_2 in mammalian cell cultures for subsequent labeling. We recently demonstrated superior stability of the receptor isolated from mammalian cell cultures due to post-translational modifications of the receptor molecule by glycosylation of its N-terminal domain and palmitoylation of C-terminal tail. (12) It is expected that higher stability of the receptor will translate into a more rigid conformation that is less susceptible to unfolding and interaction with sulfhydryl reagents. Additionally, we would like to further expand upon our EPR methodology to determine more detailed structural and environmental information about CB_2 using methods such as EPR power saturation measurements at variable oxygen concentrations and in the presence of water soluble relaxation agents (27) and distance measurements within the protein by double-electron electron resonance (DEER).

Supplementary Material

Refer to Web version on PubMed Central for supplementary material.

Acknowledgements

This work was supported by the Intramural Research Program of the NIAAA, NIH. The content is solely the responsibility of the authors and does not necessarily represent the official views of the National Institutes of Health.

References

1. Li X, Hua T, Vemuri K, Ho JH, Wu Y, Wu L, Popov P, Benchama O, Zvonok N, Locke K, Qu L, Han GW, Iyer MR, Cinar R, Coffey NJ, Wang J, Wu M, Katritch V, Zhao S, Kunos G, Bohn LM, Makriyannis A, Stevens RC, and Liu ZJ (2019) Crystal Structure of the Human Cannabinoid Receptor CB2. Cell 176, 459–467 e413 [PubMed: 30639103]
2. Xing C, Zhuang Y, Xu TH, Feng Z, Zhou XE, Chen M, Wang L, Meng X, Xue Y, Wang J, Liu H, McGuire TF, Zhao G, Melcher K, Zhang C, Xu HE, and Xie XQ (2020) Cryo-EM Structure of the Human Cannabinoid Receptor CB2-Gi Signaling Complex. Cell
3. Hua T, Li X, Wu L, Iliopoulos-Tsoutsouvas C, Wang Y, Wu M, Shen L, Johnston CA, Nikas SP, Song F, Song X, Yuan S, Sun Q, Wu Y, Jiang S, Grim TW, Benchama O, Stahl EL, Zvonok N, Zhao S, Bohn LM, Makriyannis A, and Liu ZJ (2020) Activation and Signaling Mechanism Revealed by Cannabinoid Receptor-Gi Complex Structures. Cell
4. Hurth KM, Nilges MJ, Carlson KE, Tamrazi A, Belford RL, and Katzenellenbogen JA (2004) Ligand-induced changes in estrogen receptor conformation as measured by site-directed spin labeling. Biochemistry 43, 1891–1907 [PubMed: 14967030]
5. Borbat PP, Costa-Filho AJ, Earle KA, Moscicki JK, and Freed JH (2001) Electron spin resonance in studies of membranes and proteins. Science 291, 266–269 [PubMed: 11253218]

6. Hubbell WL, McHaourab HS, Altenbach C, and Lietzow MA (1996) Watching proteins move using site-directed spin labeling. Structure 4, 779–783 [PubMed: 8805569]
7. Fanucci GE, and Cafiso DS (2006) Recent advances and applications of site-directed spin labeling. Curr Opin Struct Biol 16, 644–653 [PubMed: 16949813]
8. Hubbell WL, Cafiso DS, and Altenbach C (2000) Identifying conformational changes with site-directed spin labeling. Nat Struct Biol 7, 735–739 [PubMed: 10966640]
9. Hustedt EJ, Smirnov AI, Laub CF, Cobb CE, and Beth AH (1997) Molecular distances from dipolar coupled spin-labels: the global analysis of multifrequency continuous wave electron paramagnetic resonance data. Biophys J 72, 1861–1877 [PubMed: 9083690]
10. McHaourab HS, Kalai T, Hideg K, and Hubbell WL (1999) Motion of spin-labeled side chains in T4 lysozyme: effect of side chain structure. Biochemistry 38, 2947–2955 [PubMed: 10074347]
11. Columbus L, Kalai T, Jeko J, Hideg K, and Hubbell WL (2001) Molecular motion of spin labeled side chains in alpha-helices: analysis by variation of side chain structure. Biochemistry 40, 3828–3846 [PubMed: 11300763]
12. Yeliseev A, van den Berg A, Zoubak L, Hines K, Stepnowski S, Williston K, Yan W, Gawrisch K, and Zmuda J (2020) Thermostability of a recombinant G protein-coupled receptor expressed at high level in mammalian cell culture. Sci Rep 10, 16805 [PubMed: 33033368]
13. Yeliseev A, and Gawrisch K (2017) Expression and NMR Structural Studies of Isotopically Labeled Cannabinoid Receptor Type II. Methods Enzymol 593, 387–403 [PubMed: 28750812]
14. Stoll S, and Schweiger A (2006) EasySpin, a comprehensive software package for spectral simulation and analysis in EPR. J Magn Reson 178, 42–55 [PubMed: 16188474]
15. Etienne E, Le Breton N, Martinho M, Mileo E, and Belle V (2017) SimLabel: a graphical user interface to simulate continuous wave EPR spectra from site-directed spin labeling experiments. Magn Reson Chem 55, 714–719 [PubMed: 28078740]
16. Yeliseev AA, Wong KK, Soubias O, and Gawrisch K (2005) Expression of human peripheral cannabinoid receptor for structural studies. Protein Science 14, 2638–2653 [PubMed: 16195551]
17. Beckner RL, Zoubak L, Hines KG, Gawrisch K, and Yeliseev AA (2020) Probing thermostability of detergent-solubilized CB2 receptor by parallel G protein-activation and ligand-binding assays. J Biol Chem 295, 181–190 [PubMed: 31776188]
18. Piscitelli CL, Kean J, de Graaf C, and Deupi X (2015) A Molecular Pharmacologist's Guide to G Protein-Coupled Receptor Crystallography. Mol Pharmacol 88, 536–551 [PubMed: 26152196]
19. Ciancetta A, and Jacobson KA (2018) Breakthrough in GPCR Crystallography and Its Impact on Computer-Aided Drug Design. Methods Mol Biol 1705, 45–72 [PubMed: 29188558]
20. Xiang J, Chun E, Liu C, Jing L, Al-Sahouri Z, Zhu L, and Liu W (2016) Successful Strategies to Determine High-Resolution Structures of GPCRs. Trends Pharmacol Sci 37, 1055–1069 [PubMed: 27726881]
21. Congreve M, de Graaf C, Swain NA, and Tate CG (2020) Impact of GPCR Structures on Drug Discovery. Cell 181, 81–91 [PubMed: 32243800]
22. Roser P, Schmidt MJ, Drescher M, and Summerer D (2016) Site-directed spin labeling of proteins for distance measurements in vitro and in cells. Org Biomol Chem 14, 5468–5476 [PubMed: 27181459]
23. Van Eps N, Caro LN, Morizumi T, and Ernst OP (2015) Characterizing rhodopsin signaling by EPR spectroscopy: from structure to dynamics. Photochem Photobiol Sci 14, 1586–1597 [PubMed: 26140679]
24. Van Eps N, Altenbach C, Caro LN, Latorraca NR, Hollingsworth SA, Dror RO, Ernst OP, and Hubbell WL (2018) Gi- and Gs-coupled GPCRs show different modes of G-protein binding. Proc Natl Acad Sci U S A 115, 2383–2388 [PubMed: 29463720]
25. Manglik A, Kim TH, Masureel M, Altenbach C, Yang Z, Hilger D, Lerch MT, Kobilka TS, Thian FS, Hubbell WL, Prosser RS, and Kobilka BK (2015) Structural Insights into the Dynamic Process of beta2-Adrenergic Receptor Signaling. Cell 161, 1101–1111 [PubMed: 25981665]
26. Jeschke G (2012) DEER distance measurements on proteins. Annu Rev Phys Chem 63, 419–446 [PubMed: 22404592]
27. Nielsen RD, Che K, Gelb MH, and Robinson BH (2005) A ruler for determining the position of proteins in membranes. J Am Chem Soc 127, 6430–6442 [PubMed: 15853351]

Highlights

- Developed protocols for selective labeling of the human cannabinoid receptor CB_2
- Expressed 47 functionally active single cysteine constructs of CB_2
- Transition of CB_2 between activated and inactive conformation studied by EPR
- Structural changes in agonist vs. inverse agonist-bound CB_2 occur in IL3 and TM6

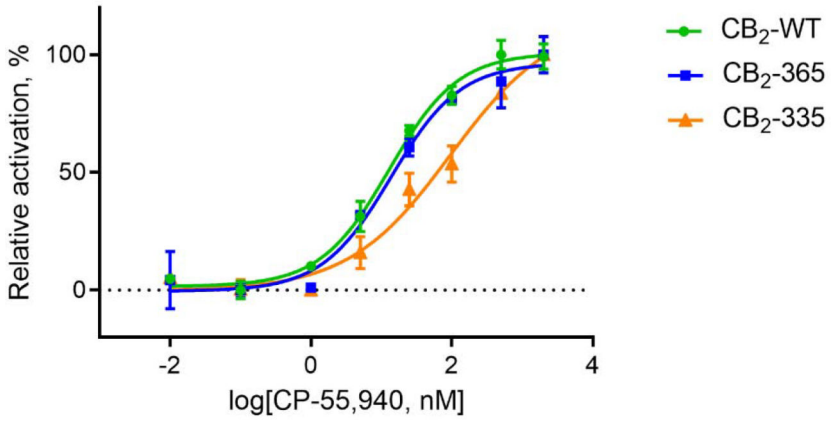

	CB2-WT	CB2-365	CB2-335
EC50	12.87	13.70	95.38

Figure 1. Functional activity of cysteine-replacement constructs of CB_2.

GEF assay of CB_2-WT and constructs CB_2-365 and CB2–335. In CB_2-365, all non-essential cysteine residues in water-exposed regions of CB_2 have been replaced C(4, 134, 175, 313, 320, 360)S. In CB_2-335, four additional cysteine residues in TM regions have been replaced (C(4, 134, 175, 313, 320, 360, 40, 89, 288)S, C284A). EC_{50} determined by titrating increasing concentrations of an agonist CP-55,940.

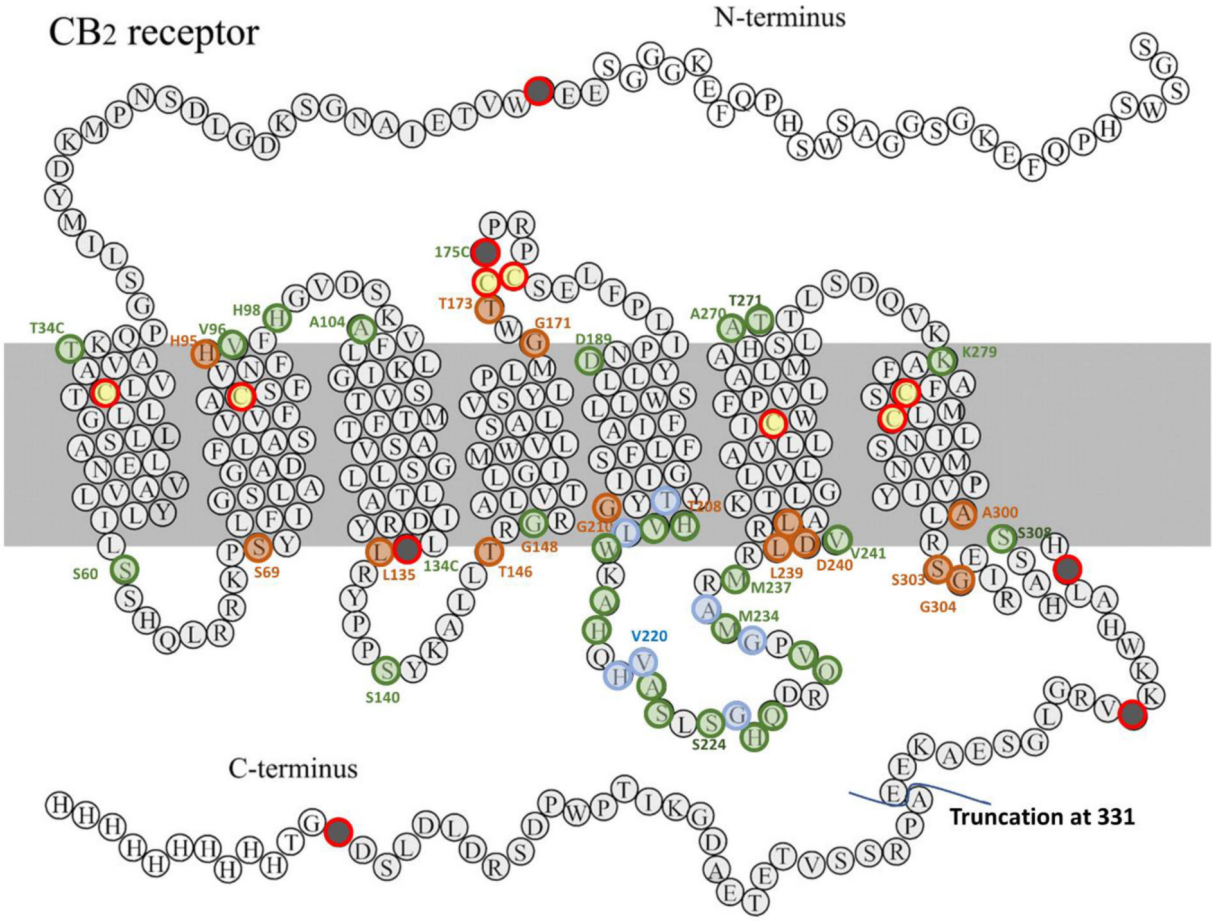

Figure 2. Snake diagram of the minimal cysteine construct and mutant series.

Green circles indicate either no decrease or a small decrease in functional activity; blue circles – moderate decrease in functional activity; brown circles – large decrease in functional activity. Red circles filled with black show the naturally occurring in the wild type cysteine residues replaced with serine residues; red circles filled with yellow - naturally occurring cysteines remaining in a construct. Each blue, green, and brown-colored circle represents a single construct where the residue was replaced with a cysteine. The relative activity of CB_2 variants was calculated as a ratio of the functional activity determined by the GEF test to the relative expression levels determined by semiquantitative Western blot.

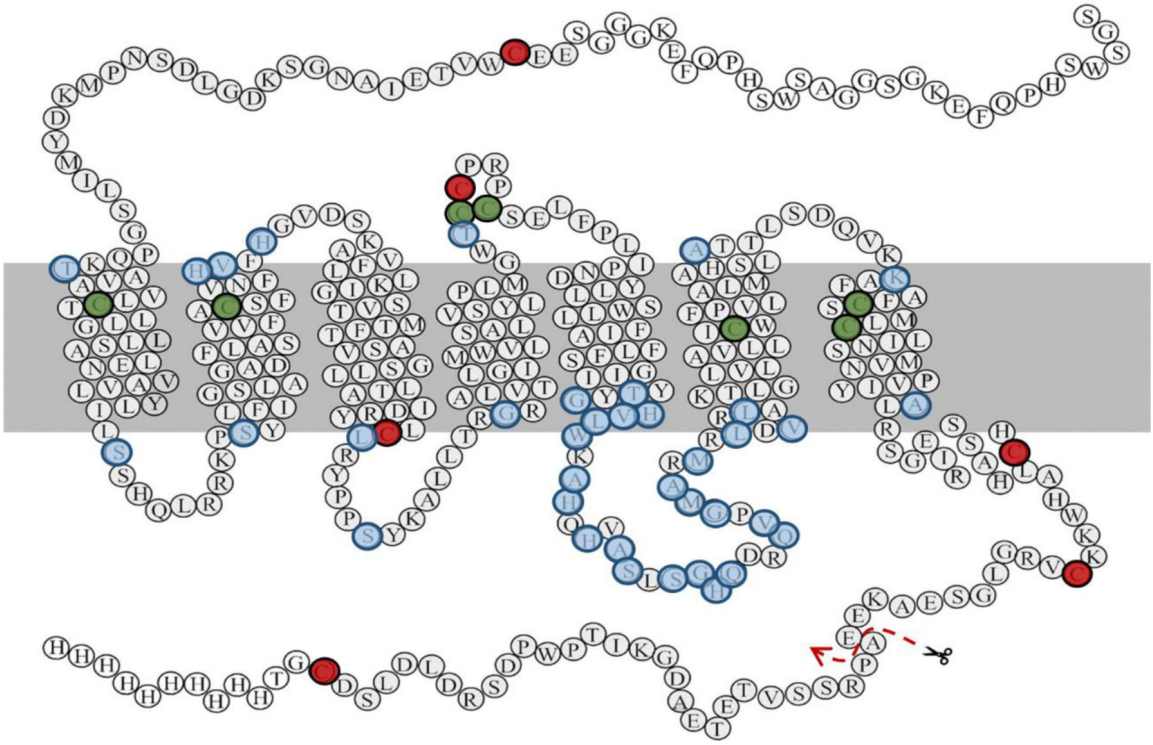

Figure 3. Snake diagram of CB_2 mutant series used for EPR labeling optimization.

Red circles represent cysteine residues that were removed from the wild type receptor. Green circles represent the wild type cysteine residues that are critical for protein function, and thus are retained in the CB_2-365. The site of truncation of the C-terminus of CB_2 C-331is shown by a dotted line. Each blue circle represents an individual variant from the CB_2-365 base construct where a single cysteine is introduced at the marked location for spin labeling. This resulted in a library of 37 individual protein variants to be used for the spin labeling.

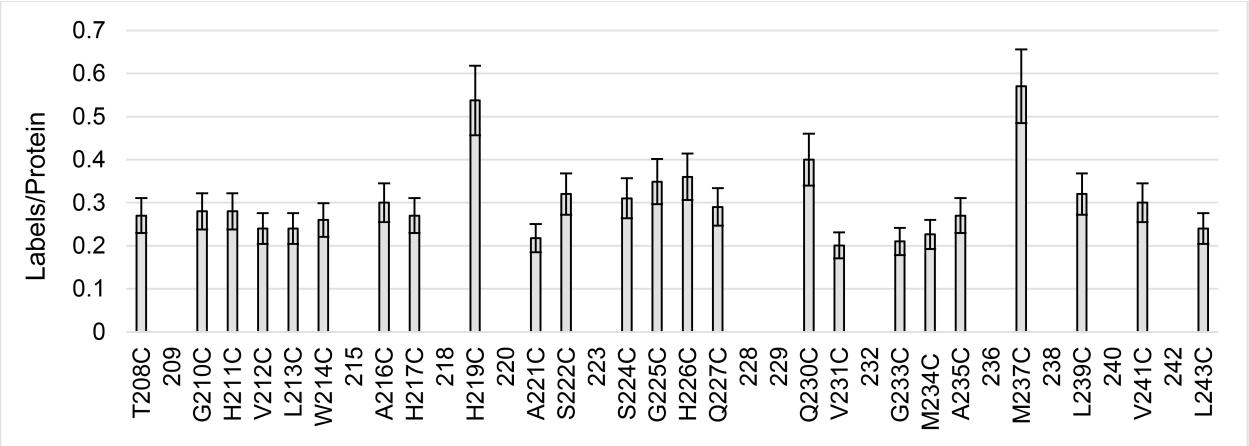

Figure 4. Labeling of variant constructs in the IL3 in the presence of inverse agonist SR-144,528.
Gaps represent the residues in the protein that were not tested in this study. Error bars represent 15% variation due to error limits of EPR measurement and protein concentration measurement for each individual sample.

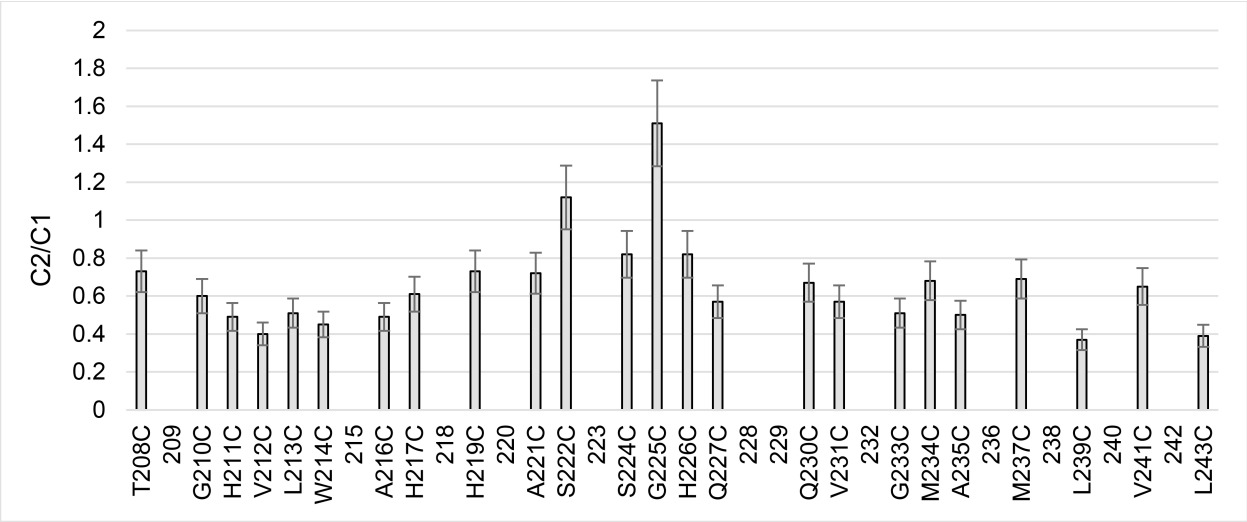

Figure 5. Ratio of Component 2/ Component 1 of IL3 constructs.

EPR analysis of CB_2 variant proteins from the minimal cysteine series bound to SR-144,528 ligand. Component 1 parameter values indicate more immobilized movement of the spin label, while the Component 2 parameter values indicates higher mobility of the spin label. The C2/C1 ratio reports the overall mobility of the labeled site.

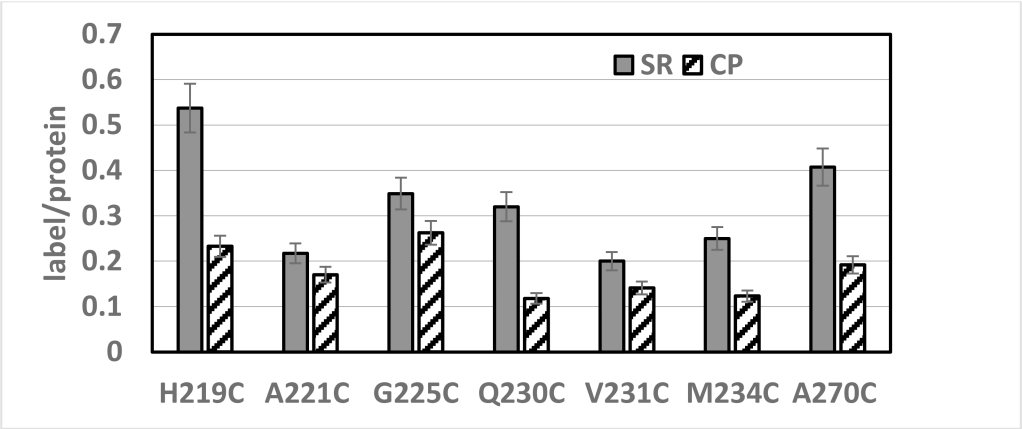

Figure 6. Comparison of select sites in IL3.

Select CB_2 mutants bound to SR-144,528 or CP-55,940 were compared using EPR analysis. The labels/protein values of these mutants are compared. For comparison, the site A270C is also shown. Error bars represent 15% variation due to error limits of EPR measurements and protein concentration measurement for each individual sample.

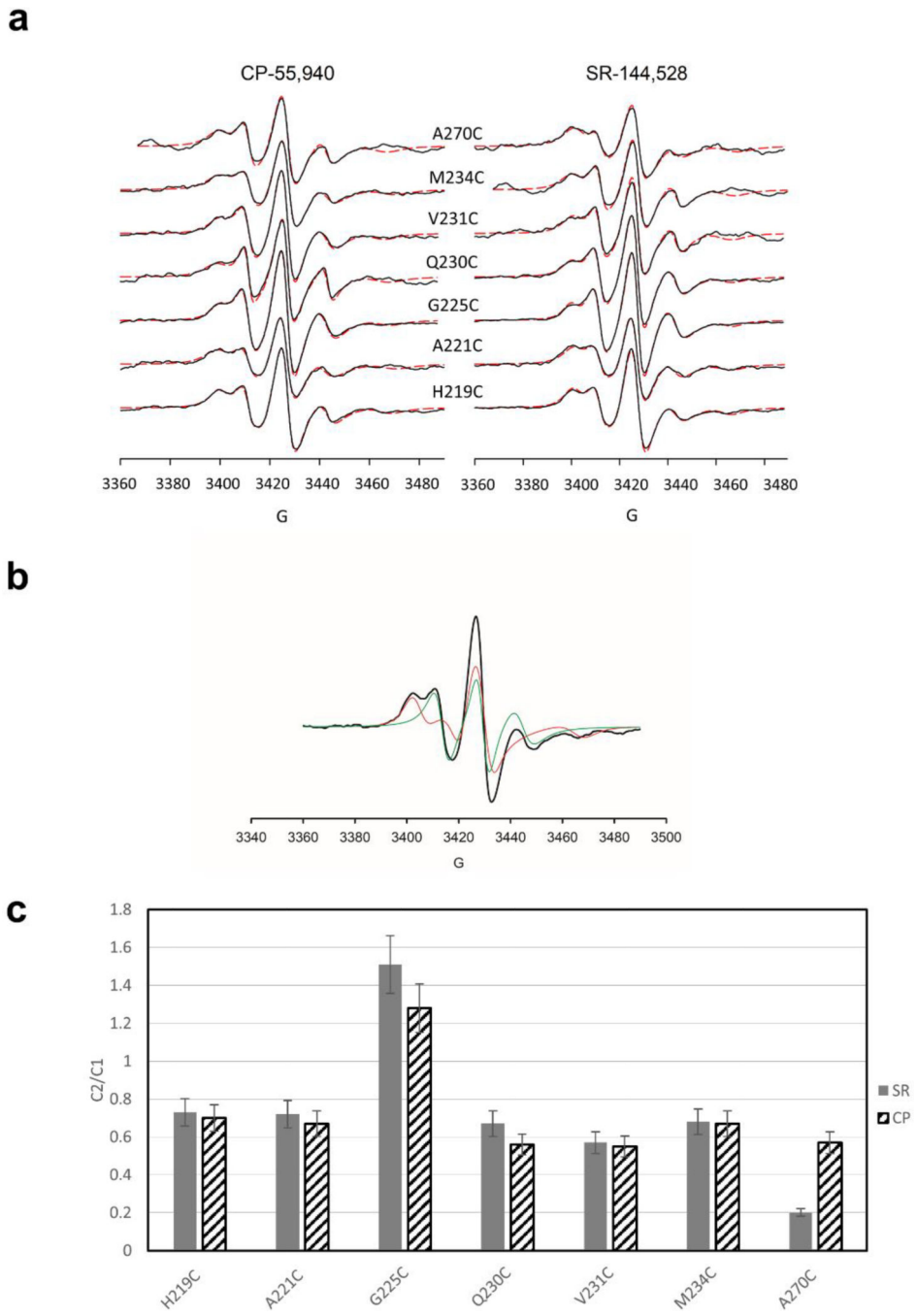

Figure 7. Comparison of inverse agonist-bound (SR-144,528) and agonist-bound (CP-55,940) CB_2 mutants.

a. Experimental EPR spectra for CB_2 mutants labeled with IA-Proxyl spin label. Black traces are the experimental spectra and the red traces represent the generated spectral fit. **b**. Experimental spectrum (black) of sample H219C (SR-144,528) with spectra of fitted component 1 (red) and component 2 (green). **c**. The C2/C1 ratios derived from fitting.